JOURNAL OF MATERIALS SCIENCE 33 (1998) 1907–1914

Development of a new forming method (pressureless powder packing forming method) and its characteristics

J. H. PARK, J. S. SUNG, K. S. YOUM
Department of Ceramic Engineering, Yonsei University, 134 Shinchon-dong, Sudaemoon-ku, Seoul, Korea
E-mail: sungjs@nuri.keti.re.kr

In order to form ceramics of complex shape with simple steps the new process was developed and its characteristics were investigated. The main concepts of this process were powder packing by vibration and the infiltration of binder solution into packed powder. By using this method, it is possible to fabricate homogeneous, porous and complex-shaped ceramics. © *1998 Chapman & Hall*

1. Introduction

Conventional forming techniques are roughly classified as pressing, casting and plastic forming methods [1]. Dry pressing is a widely used method because of its simplicity but it has some disadvantages, namely that residual stress within the green body can be produced and fabrication of a complex shape is difficult [1–3]. Also damage to the press die can occur in the case of forming with hard and irregular particles. In casting and plastic forming [4, 5], ceramic powders are mixed with many polymeric additives, and green bodies are made of these slurry (plastic) states. However, these processes also have some disadvantages such as the complex processing step, the limitation of usable powders, and the existence of a large quantity of polymeric additives within the green body.

In order to solve these problems in the forming process, a new forming method, the pressureless powder packing (PLPP) forming method, was developed and various alumina powders were applied to this process. From these experiments, the aim of this paper is to characterize this new method and to investigate its field of application.

2. Pressureless powder packing forming method

A schematic diagram of this method is shown in Fig. 1. To reduce the stress gradient within the green body and to increase the shape capability, this process contained the following steps. Powders were packed into the mould by mechanical vibration without any pressing, the binder solution was infiltrated into the packed powder and, after drying, the green body was obtained. In this method, the capillary produced by pores between packed powders was the driving force for binder infiltration, and, to demould the green body easily and to form a complex shape, silicone rubber was used as the mould material. Studies on powder packing have already been carried out long ago [6, 7], but this was only work about the properties of powder in itself. Infiltration phenomena have been widely investigated topics in the fabrication of ceramics [8–10]. These packing and infiltration concepts were introduced

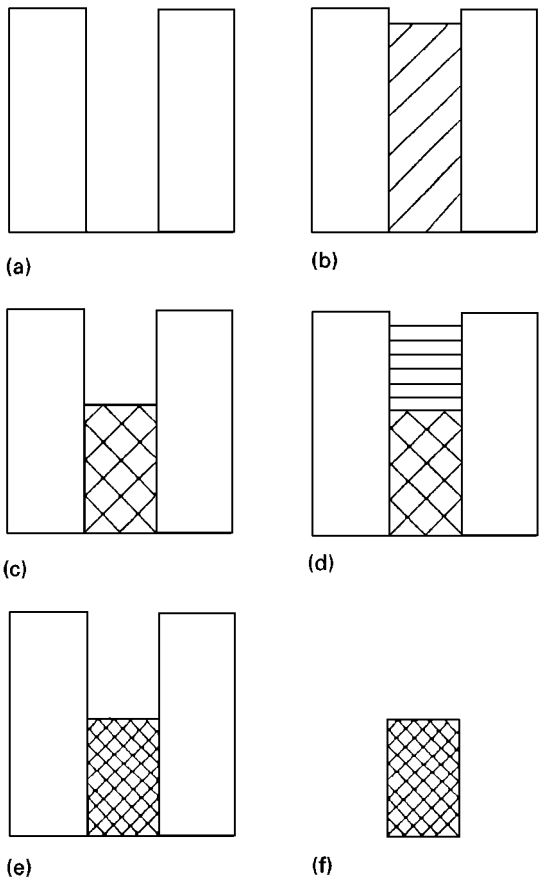

Figure 1 Schematic diagram illustrating the PLPP forming method. (a) silicone rubber mould; (b) pouring powder; (c) packing by vibration; (d) infiltration of binder solution; (e) drying; (f) green body.

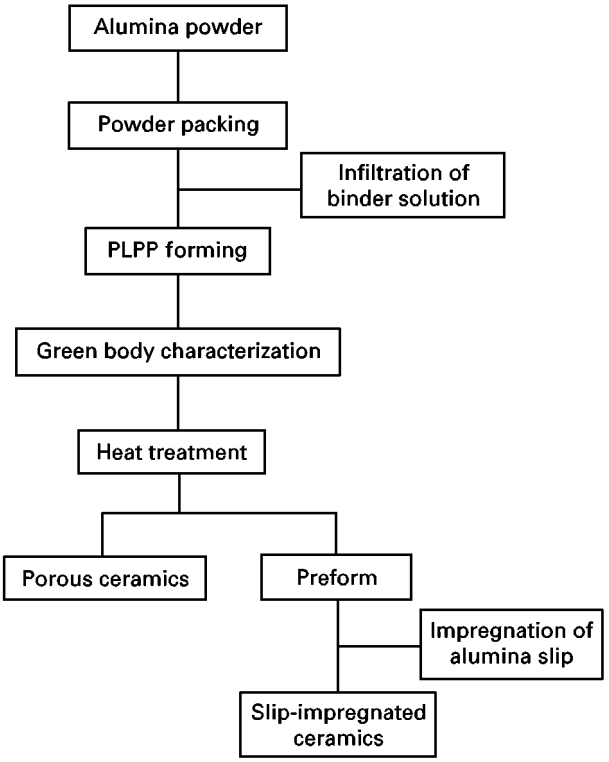

Figure 2 Overall experimental flow chart.

into this forming method and, in using this new process, a homogeneous green body, fabrication of complex shapes, easy forming of hard and irregularly shaped particles and a reduction in cost because of the simple steps can be expected.

3. Experimental procedure

Fig. 2 shows an overall flow chart of this experiment. Five kinds of alumina powder with different particle sizes and shapes were used as starting materials and, to prevent agglomeration due to humidity, all powders were dried in an oven at 200 °C for 24 h, and their packing densities were measured. In this forming, methyl cellulose solution (0.5 wt%) was used as binder, and the green densities were measured and compared with those of dry-pressed (60 MPa) specimens.

The binder distribution of the green body was observed in the vertical and radial directions from the weight loss of each part of the specimen after heating and the sintered densities were assessed by the Archimedes method in distilled water.

Sintering was performed at several temperatures (1100–1700 °C) for 2 h; the pore size distribution of the specimen was measured with a mercury porosimeter (Autopore II 9220 V 1.05).

In order to increase the sintered density, alumina slip was impregnated into the preform and the microstructure were observed by scanning electron microscopy (SEM) (JEOL, JSM 35-CF, Japan).

4. Results and discussion

The characteristics of the five kinds of alumina used in this experiment are given in Table I, and Fig. 3 shows their particle shapes. CA powders are illustrated in their aggregate state and SD1 showed a smaller, more spherical granule than SD2, and the primary particle sizes of these granules were the same (about 4 μm). FA are fused alumina powders (−220 mesh), and PM mixed powders of fused aluminas with different particles sizes (−100, −220 and −320 mesh) with a high packing density.

TABLE I Characterization of alumina powder used in this experiment

Alumina powder	Average particle size (μm)	Particle shape	Packing density (g cm^{-3} (%))
Calcined Al_2O_3, CA	≈ 18	Round	1.06 (26.6)
Calcined Al_2O_3, SD1	≈ 25	spherical	1.25 (31.4)
Calcined Al_2O_3, SD2	≈ 85	Hollow spherical	1.23 (30.9)
Fused Al_2O_3, FA	≈ 8	Angular	2.05 (51.2)
Fused Al_2O_3, PM	≈ 11	Angular	2.39 (60.2)

From the result of the packing densities shown in Table I, it was found that fused alumina powders exhibited higher packing densities and PM showed the highest density. This resulted from the fact that fused powders had no micropores within individual particles and mixed powders showed effective packing because of the mixing effect of different particle sizes [11, 12].

Table II shows a comparison between the green densities of these green bodies and those of dry-pressed specimens. Of the five types of specimen, SD1 and SD2 were formed by the infiltration of only water, and not binder solution, because the granule had already contained binder from the spray-drying process and this binder was water soluble. The green densities were a little higher than the packing densities because slight shrinkages occurred during the drying process; because there was no pressurization step the green densities were lower in comparison with those of the dry-pressed specimens. These differences decreased for the fused alumina specimens, and in particular for the PM specimen these densities were nearly the same. It was thought that the high packing density of fused alumina powders and ineffectiveness of the pressing process owing to the irregular particle shape caused the densities to be similar. From these results it was found that this method was effective in forming irregular and hard particles.

The result of the binder distribution within this green body (Fig. 4) illustrated that binders were homogeneously distributed in the vertical direction and a homogeneous binder distribution was also shown in the radial direction (Fig. 5). Although the amount of binder was small (below 1 wt%), the green strength was sufficient for handling owing to its homogeneous binder distribution.

Fig. 6 is a photograph of ceramics of various shapes formed by this new process, such as turbocharger rotor, tube and disc, and it was found that it was possible to fabricate more complex-shaped ceramics.

The fracture surfaces of green bodies and sintered bodies heated at 1700 °C for 2 h are shown in Fig. 7

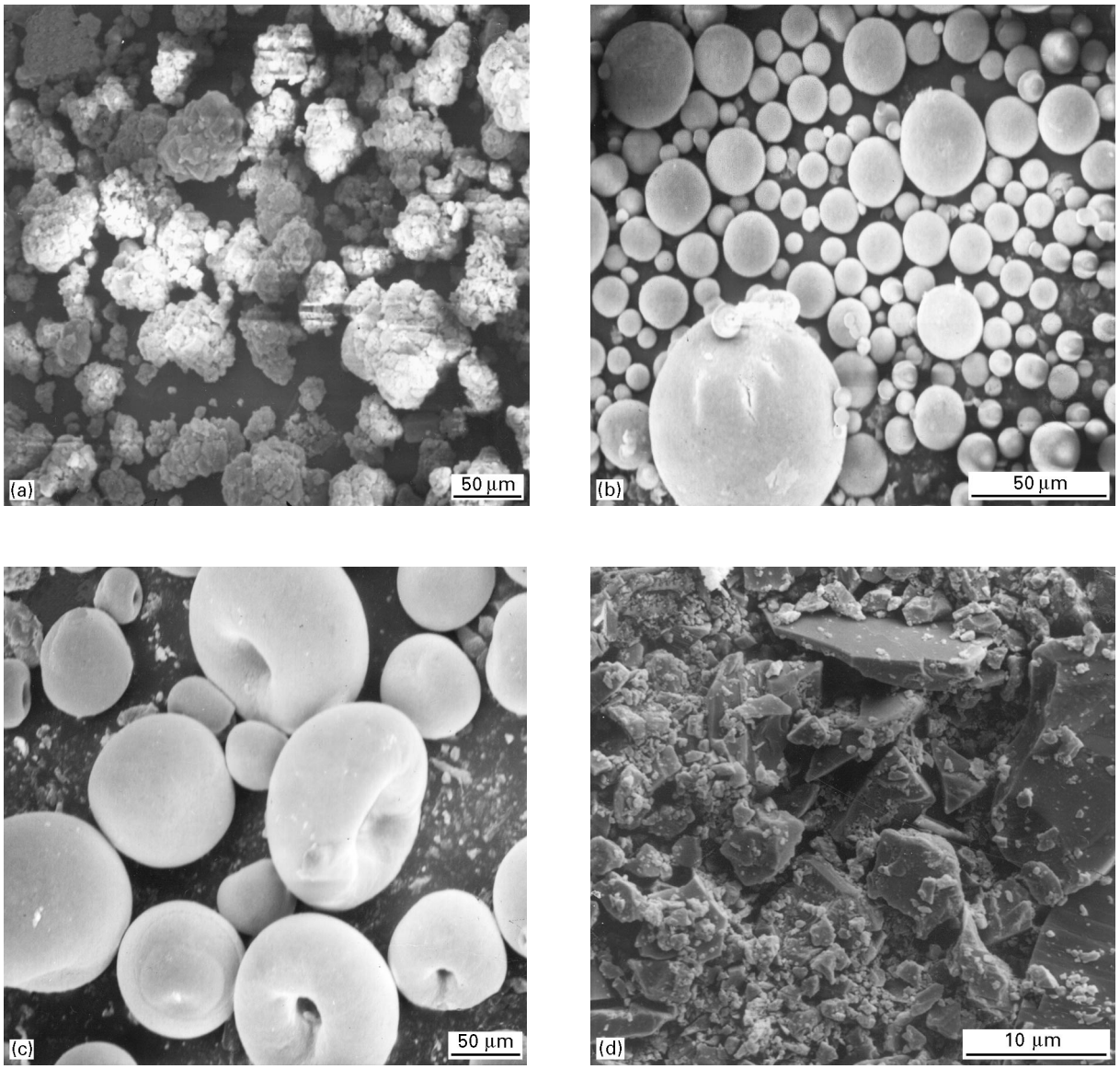

Figure 3 SEM photographs of starting alumina powders: (a) CA; (b) SD1; (c) SD2; (d) FA; (e) PM.

and the data on the sintered densities are given in Table III. In all specimens the sintered densities were low owing to their low green densities. The PM specimen had a density similar to that of the dry-pressed specimen because it had a high packing density and green density.

SEM of the fracture surface showed that the starting granules were not deformed and fractured, which generally occurs in dry pressing [13]. Therefore, it was thought that these specimens showed a special sintering mechanism, namely that primary particles within granules were densified and necking between granules also occurred. Specimens SD1 and SD2 had the same primary particles but the shapes and sizes of the granules were different. Although the differences between the packing densities of the two specimens were small the sintered density of SD1 was much higher than that of SD2. It was thought that this phenomenon was caused by the shape effect, i.e., shrinkage of granules occurred in the drying process and the effect of pores in the centre of a hollow granule of SD2 became relatively large. From this result, the green density of SD2 was lower than that of SD1 and, because this shrinkage effect had a very serious influence during the heat treatment, the sintered density of SD2 was lower.

TABLE II Comparison of green densities for different forming methods

Alumina powder	Green density (g cm^{-3} (%))	
	PLPP forming	Dry pressing
CA	1.08 (27.3)	1.65 (41.6)
SD1	1.48 (37.3)	2.18 (54.9)
SD2	1.28 (32.2)	2.22 (55.9)
FA	2.17 (54.6)	2.63 (66.2)
PM	2.40 (60.6)	2.49 (62.8)

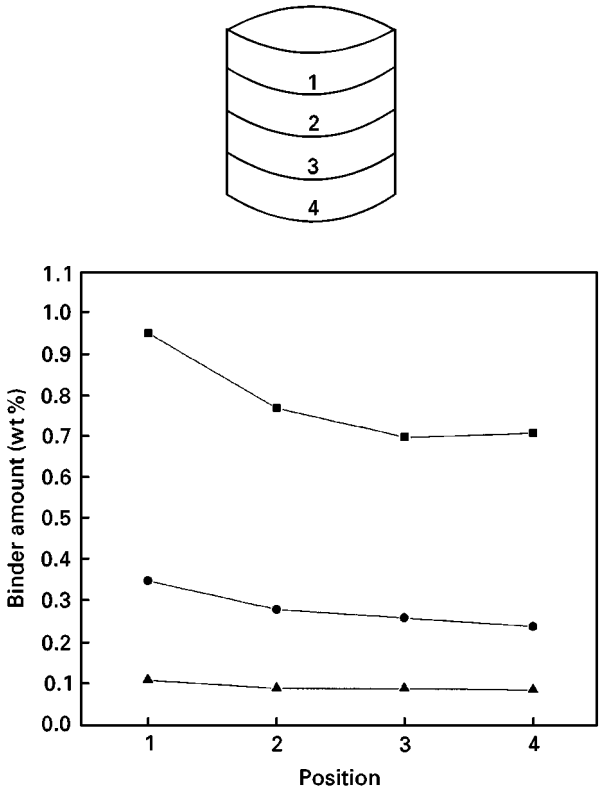

Figure 4 Binder distribution in the green body formed by the PLPP forming method (vertical direction) (■), CA; (●), FA; (▲), PM.

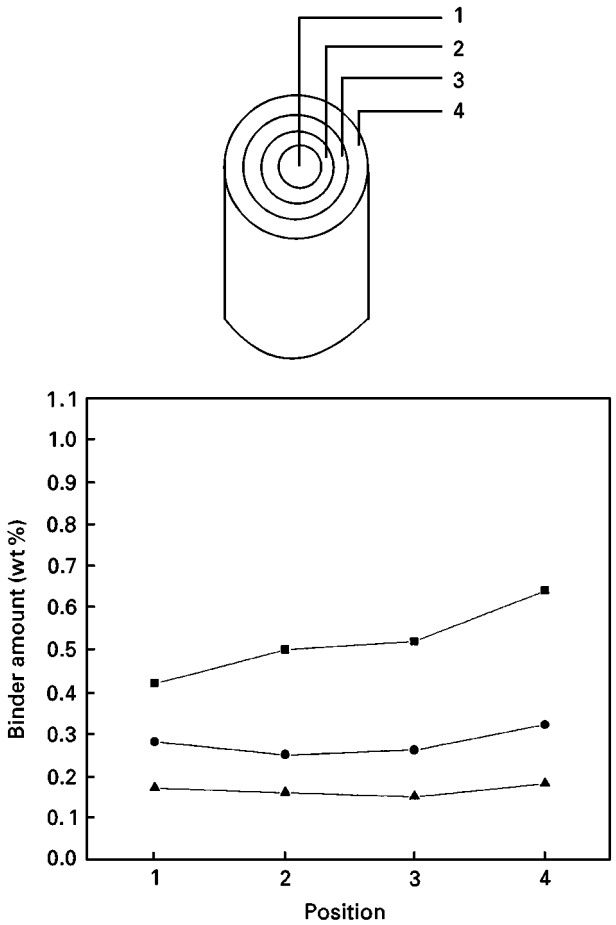

Figure 5 Binder distribution in the green body formed by PLPP forming method (radial direction). (■), CA; (●), FA; (▲), PM.

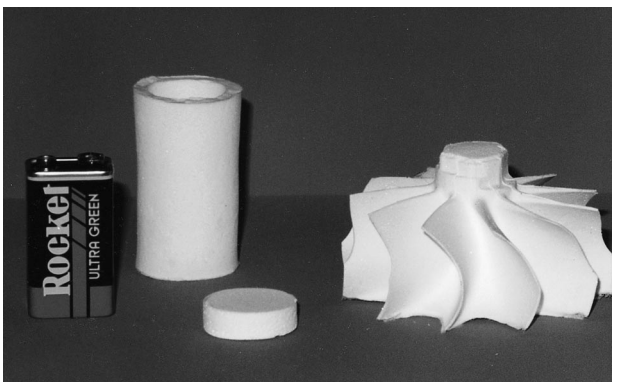

Figure 6 Various green bodies formed by the PLPP method.

The results of pore size distribution are shown in Figs 8 and 9. At low heating temperatures it was observed that large and small pores coexisted (Fig. 8a). This pore size distribution mean that small pores produced by primary particles, and large pores produced by granules, coexist because the heating temperature was below sintering temperature of the primary particles. As the heating temperature increased, densification progressed and a bimodal distribution clearly occurred. At 1700 °C, small pores disappeared and only large pores (about 4 μm) were distributed homogeneously. Fig. 8d shows that SD2 had larger pores (about 15 μm) than SD1 did because of its hollow shape, and the narrow pore size distributon should also be noted. In general, because the hollow shape of granules may produce a low green density in dry pressing [13], this shape was excluded. However, where a porous material is required, using this new forming, hollow-shaped granules could be usable for large pore sizes and porosity. Fig. 8e shows the result for a dry-pressed specimen heated at 1100 °C. It was thought that granules were fractured during pressing; so only small pores resulting from primary particles existed. Specimens FA and PM (Fig. 9) also showed uniform pore size distributions and the shapes of the distributions were similar to that of dry-pressed specimens.

From these results, it was found that the fabrication of uniform and porous ceramics can be obtained using this forming method. In particular, when the particles are hard and angular (such as fused alumina) this

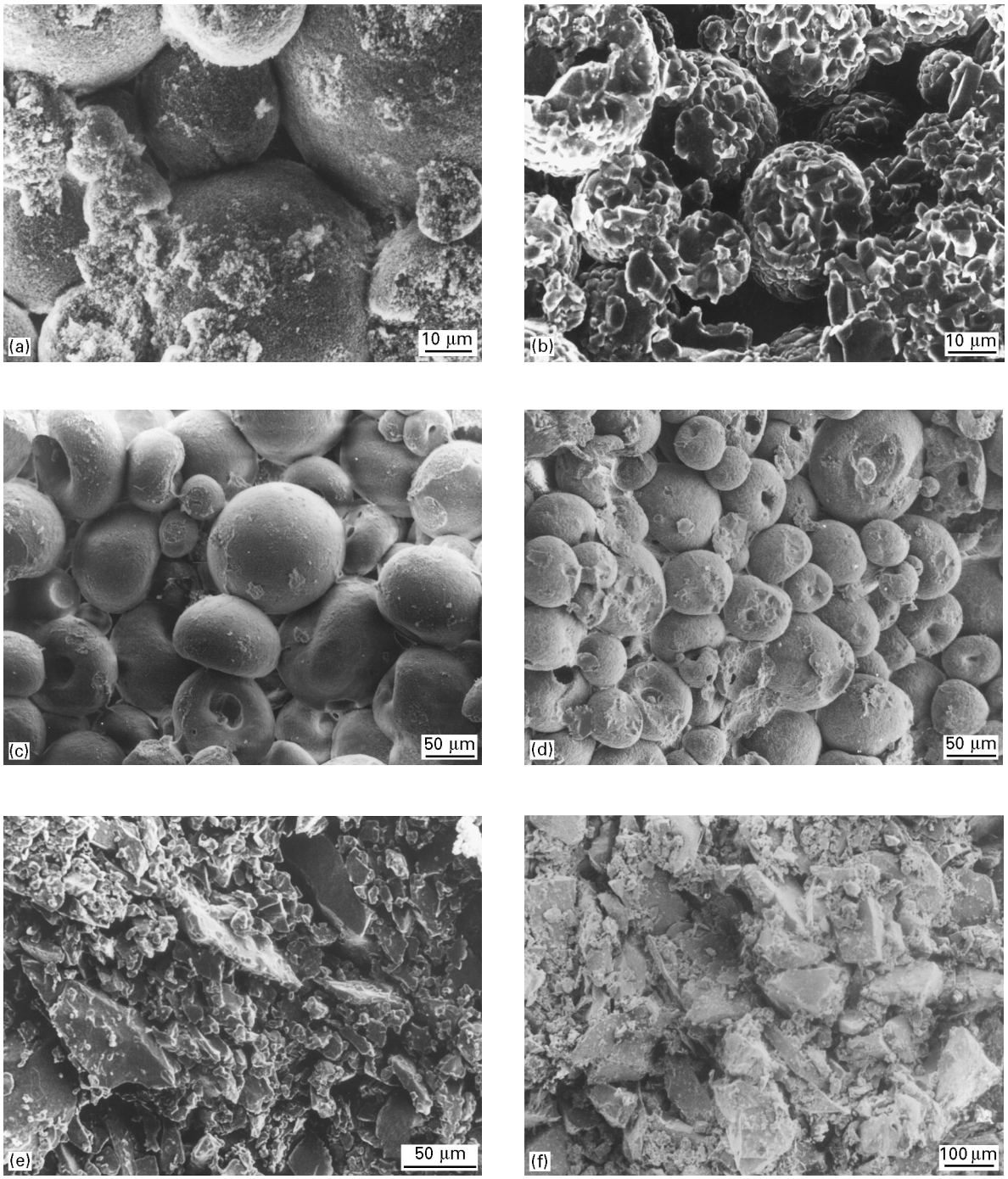

Figure 7 SEM photographs of the fracture surface: (a) green body of SD1; (b) sintered body of SD1; (c) green body of SD2; (d) sintered body of SD2; (e) sintered body of FA; (f) sintered body of PM.

TABLE III Comparison of sintered densities for different forming methods

Alumina powder	Sintered density (g cm^{-3} (%))	
	PLPP forming	Dry pressing
CA	2.04 (51.2)	2.87 (72.1)
SD1	2.96 (74.5)	3.82 (96.2)
SD2	2.46 (61.8)	3.80 (95.7)
FA	2.43 (61.6)	2.82 (70.9)
PM	2.52 (63.4)	2.63 (66.3)

forming method is easier than dry pressing, and the sintered densities are about the same. When granules are used in forming, this process is an effective way to fabricate porous ceramics. That is to say, the starting granule state is not deformed or fractured during the forming and sintering step; so the porosity and pore size can be simply controlled by varying the size and shape of the granules. Also this porosity and pore size are maintained at high temperatures; so a high thermal stability can be obtained.

In addition, to increase the sintered density, a slip impregnation process was introduced; specimen SD2 with a high porosity was employed as a preform and two different slips (alumina: water = 2:1 and 1:1

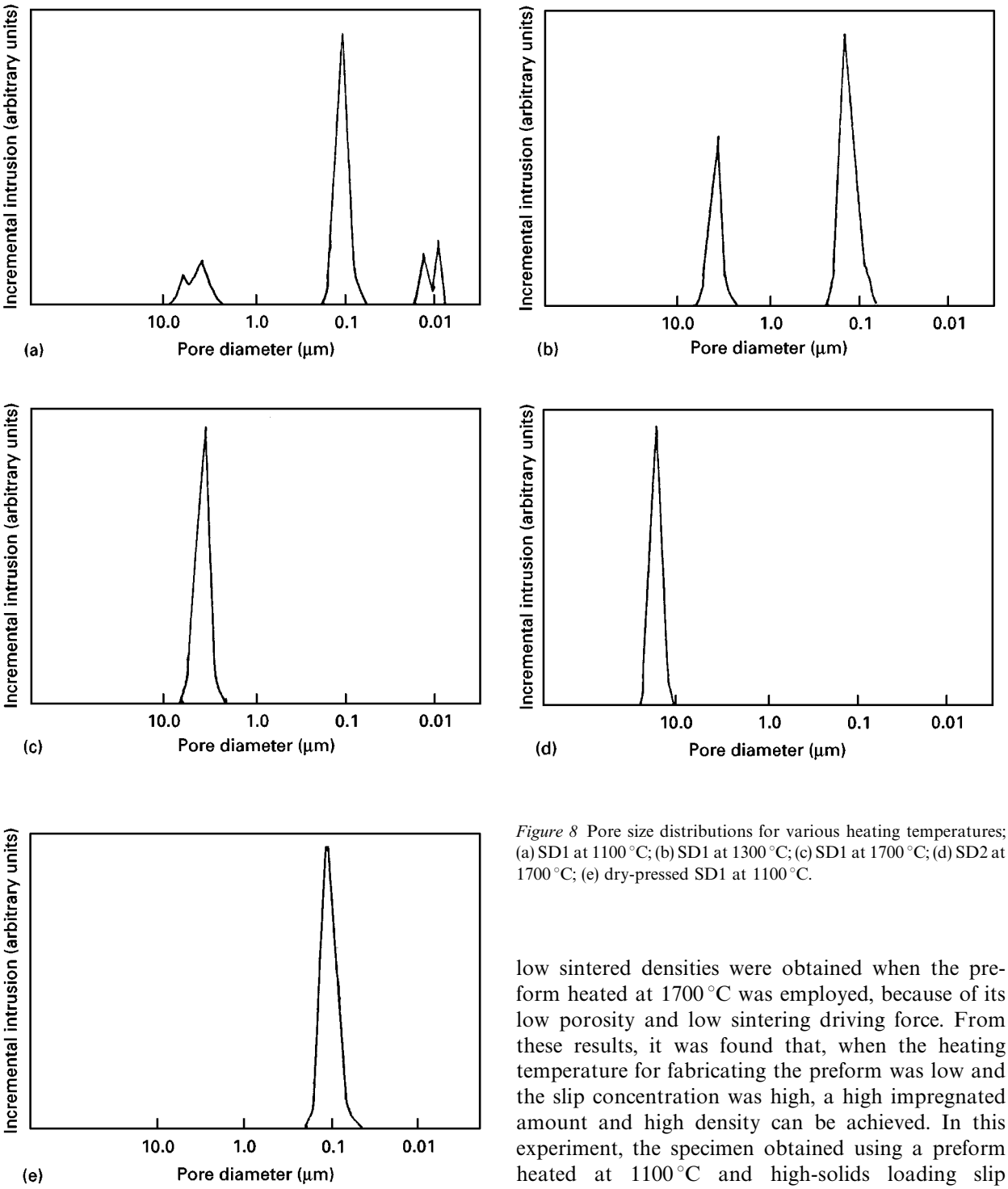

Figure 8 Pore size distributions for various heating temperatures; (a) SD1 at 1100 °C; (b) SD1 at 1300 °C; (c) SD1 at 1700 °C; (d) SD2 at 1700 °C; (e) dry-pressed SD1 at 1100 °C.

(wt%) were used in this experiment. The impregnation apparatus was designed to obtain the reduction pressure, impregnation of slip and pressurization within the chamber (5 kgf cm^{-2}) and a diagram is shown in Fig. 10. In this study the SD2 preforms were fabricated by heating at 1100 °C and 1700 °C and their densities were 34% and 61.8%, respectively.

Table IV shows the results of impregnated amounts and sintered densities of impregnated specimens. When using a high-solids loading slip (alumina:water, 2:1), the impregnated amount was higher than that using a low-solids loading slip (alumina:water, 1:1); low impregnated amounts and low sintered densities were obtained when the preform heated at 1700 °C was employed, because of its low porosity and low sintering driving force. From these results, it was found that, when the heating temperature for fabricating the preform was low and the slip concentration was high, a high impregnated amount and high density can be achieved. In this experiment, the specimen obtained using a preform heated at 1100 °C and high-solids loading slip (alumina:water, 2:1) showed high impregnation (25.2%) and high sintered density (82.8%) comparatively, and this amount of impregnation was close to the amount (31.7%) theoretically calculated by considering perfect filling of alumina slip into pores; therefore it was found that effective impregnation can occur and a higher density can be achieved.

5. Conclusion

A new forming process has been developed and its characteristics were investigated. A homogeneous binder distribution within the green body was observed and complex-shaped ceramics can be fabricated easily and simply. Forming with fused alumina powder is easier than the dry-pressing method; in particular, when granules were used in this forming,

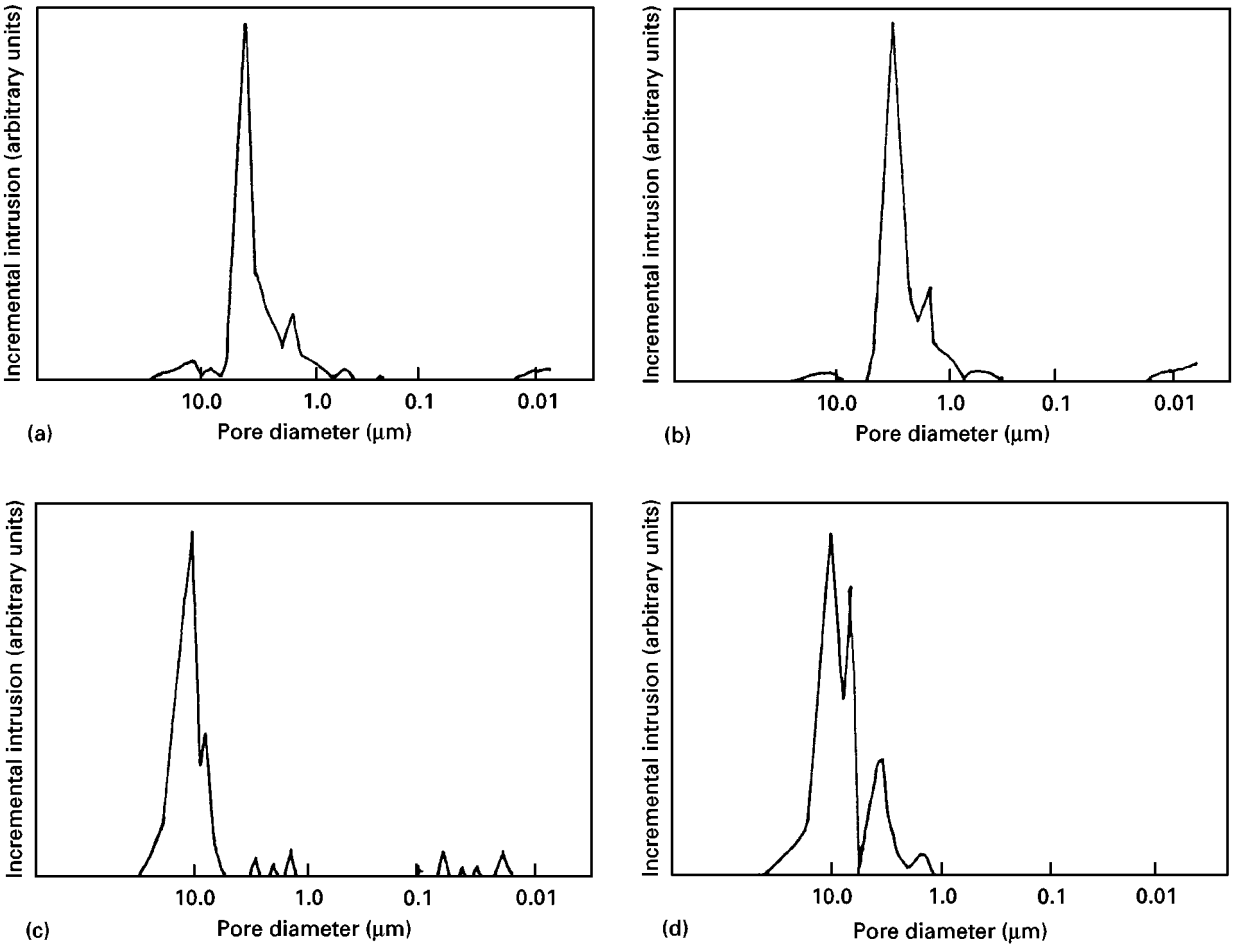

Figure 9 Pore size distributions for the two forming methods; (a) FA formed by PLPP forming at 1700 °C; (b) FA formed by dry pressing at 1700 °C; (c) PM formed by PLPP forming at 1700 °C; (d) PM formed by dry pressing at 1700 °C.

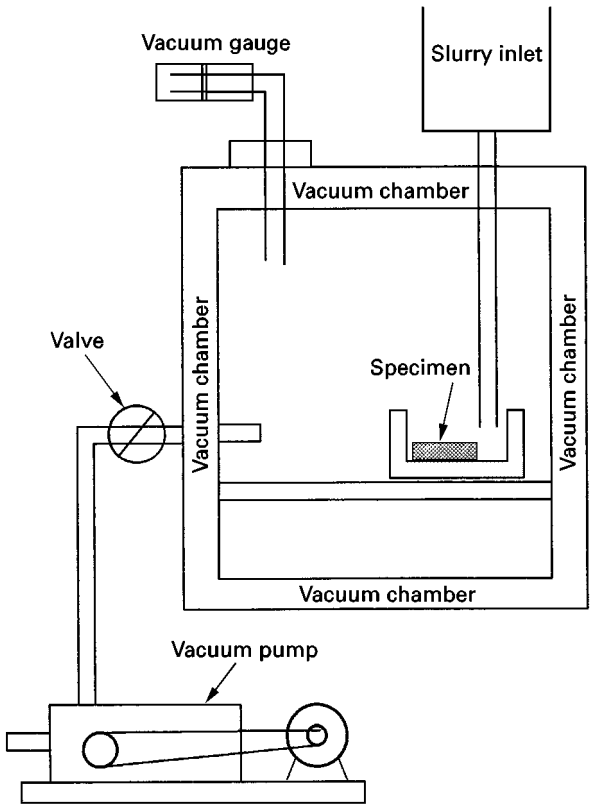

Figure 10 Schematic diagram of the impregnation apparatus.

TABLE IV Infiltrated amounts and sintered densities with slip conditions and preform conditions

Preform[a] condition, i.e., pre-heating temperature (°C)	Slip condition (alumina:water)	Infiltrated amount (wt%)	Sintered density (%)
1100	1:1	12.4	74.1
1100	2:1	25.2	82.8
1700	2:1	16.3	76.9

[a] The preform is fabricated with SD2.

this process was very effective for fabricating porous ceramics because no deformation and fracture of the granule state occurred. From these results, by using this new forming method, it was found that it was possible to fabricate homogeneous ceramics and to achieve an increase of density to some extent through the slip impregnation process. Therefore, this method can be applied to porous and complex-shaped ceramics with a high thermal stability, microfiltration membranes, refractory blocks, etc.

Acknowledgements

This work was carried out with the support of the Ministry of Education Research Fund for Advanced Materials in 1994 and the author gratefully acknowledges for this.

References

1. D. W. RICHERSON, in "Modern Ceramic Engineering" (Marcel Dekker, Cambridge, 1990) 2nd Edn, p. 418.
2. H. THURNAUER, in "Ceramic Fabrication Process" (MIT Press, Cambridge, MA, 1963) p. 62.
3. I. J. McCOLM and N. J. CLARK, in "Forming, Shaping and Working of High-performance Ceramics" (Blackie, London, 1988) p. 146.
4. J. S. REED, "Introduction to Principles of Ceramic Processing" (Wiley–Interscience, New York, 1988) p. 380.
5. G. C. ROBINSON, "Ceramic Processing Before Firing", edited by G. C. ONODA and L. L. HENCH (Wiley–Interscience, New York, 1978) p. 391.
6. A. E. R. WESTMAN and H. R. HUGILL, *J. Am. Ceram. Soc.* **13** (1930) 767.
7. R. K. McGREARY, *J. Am. Ceram. Soc.* **44** (1961) 513.
8. M. S. NETUT, A. W. URGUHART and H. R. ZWICKER, *J. Mater. Res.* **1** (1986) 81.
9. V. BELTRAN, A. BARBA, J. C. JARGUE and A. ESCARDING, *Brit. Ceram. Trans.* **90** (1991) 77.
10. M. M. SCHWARTZ, "Composite Materials Handbook" (McGraw-Hill, New York, 1992) p. 491.
11. F. N. RHINES, "Ceramic Processing Before Firing", edited by G. C. ONODA and L. L. HENCH (Wiley–Interscience, New York, 1978) p. 321.
12. J. S. REED, "Introduction to Principles of Ceramic Processing" (Wiley–Interscience, New York, 1988) p. 185.
13. S. J. LUKASIEWICZ and J. S. REED, *Ceram. Bull.* **57** (1978) 798.

Received 5 July 1996
and accepted 22 August 1997